Neurosurgical Review (2022) 45:3381–3391
https://doi.org/10.1007/s10143-022-01846-9

RESEARCH

The medial wall and medial compartment of the cavernous sinus: an anatomic study using plastinated histological sections

Kaili Shi[1] · Zhifan Li[1] · Xiao Wu[2] · Chunjing Ma[1] · Xingyu Zhu[1] · Liu Xu[1] · Zhengzheng Sun[1] · Shengchun Xu[1] · Liang Liang[1]

Received: 29 March 2022 / Revised: 20 July 2022 / Accepted: 10 August 2022 / Published online: 19 August 2022

Abstract

The medial wall of the cavernous sinus (CS) has a significant role in evaluation and treatment of pituitary adenomas. This study was conducted to clarify the fine architecture of the medial wall and medial compartment of the CS at both macro- and micro-levels in twenty-one human cadaveric heads by using the epoxy sheet plastination technique. The sellar part medial wall is an intact dural layer that separates the CS from the pituitary gland. This dural wall adhered to the diaphragma sellae and the periosteum of the sella turcica to form fibrous triangles. Eight micro-protrusions of the pituitary gland were found at both sides of that wall. The thickness of the sellar part medial wall at its central portion was significantly thinner than that at the other surrounding portions. From the superior view, tortuous intracavernous carotid arteries can be divided into outward bending type and inward bending type. The inward bending intracavernous carotid was apt to bent towards the central part of the sellar part medial wall, where there were usually wide and short fibrous bands with more densely stained connective tissues between them. The micro-protrusion of the pituitary gland in the medial wall of the CS could provide an anatomical basis for the occult tumor invasion and the recurrence of residual tumor. Different bending facing states of tortuous intracavernous carotid arteries in the lateral direction may be a factor of the determination of the direction of growth of pituitary tumors.

Keywords Cavernous sinus · Medial wall · Dura mater · Plastination

Introduction

The cavernous sinus (CS) is a paired dural-lined venous plexus located on each side of the sella turcica at the central skull base [1–3]. The CS was described as having 4, 5, or 6 walls in several studies [1, 3–5]. The medial wall of the CS forms the medial limit of the CS and the lateral border of the pituitary fossa, which can be divided into two parts: the sellar and the sphenoidal [5].

Pituitary adenomas may infiltrate the adjacent medial wall and often invade the CS [6, 7]. However, some giant pituitary tumors do not invade into or transgress, but only compress the medial wall of the CS [8]. In addition, several recent studies have found that there were occult medial wall invasions among the patients with Knosp Grade 0 but without intraoperative apparent medial wall involvement [9, 10]. Thus, in order to achieve a low recurrence rate, it should be advocated to remove the medial wall of the CS after adenomectomy, especially in patients with functional tumors [9]. But due to the intimate relationship of the medial wall to important neurovascular structures, surgical removal of the medial wall remains a challenge, and it was advised to be performed by very experienced neurosurgeons with sufficient anatomic knowledge [6, 7, 9]. Nevertheless, there has been an ongoing debate as to the nature and architecture of the medial wall of the CS [1, 5, 7, 11–24]. Some reports even suggested that there was no a dural medial wall between the pituitary fossa and the CS [14, 17].

Therefore, the purpose of this study was to investigate the fine architecture of the medial wall and medial compartment of the CS by using the epoxy sheet plastination technique.

Kaili Shi, Zhifan Li, and Xiao Wu have contributed equally to this work.

✉ Liang Liang
liangliang@ahmu.edu.cn

[1] Department of Anatomy, School of Basic Medical Sciences, Anhui Medical University, NO. 81, Meishan Road, Shushan District, Hefei 230032, Anhui, China

[2] Department of Neurosurgery, The First Affiliated Hospital of Nanchang University, Nanchang, China

Materials and methods

A total of 21 formalin-embalmed cadaveric heads (3 females and 18 males; aged range, 35–80 years; average age at death, 58 years) were examined in this study. The cadavers were donated for anatomic education and research to the Department of Anatomy at Anhui Medical University. This study was performed in line with the principles of the Declaration of Helsinki and was approved by the Ethics Committee of Anhui Medical University.

Epoxy sheet plastination

In 9 of the 21 specimens, the whole heads were frozen and then sectioned serially to 3 mm thickness slices using a bandsaw. According to the E12 plastination technique, these frozen slices were dehydrated (− 25 °C) and degreased (room temperature) in acetone, impregnated with a resin mixture of E12/AE20/E1 (Biodur, Heidelburg, Germany), and cured at oven (45 °C). These 3 mm thickness transparent plastinated slices were used for gross anatomical observation.

The central skull base tissue blocks (approximate 10 cm × 10 cm × 10 cm in size) were sawed and removed en bloc from the remaining 12 cadaveric heads. They were plastinated using the E12/E6/E600 resin (Biodur, Heidelburg, Germany) ultra-thin plastination technique. These undecalcified resin blocks were serially sectioned in the axial (5 sets) and coronal (7 sets) planes with the Exakt 310 CP cutting system (Exakt, Norderstedt, Germany). The thickness of the ultra-thin plastinated sections was 200 ~ 300 μm. All sections stained with Stevenel's blue and Alizarin red S were examined and scanned with the TissueFAXS PLUS imaging system (TissueGnostics, Vienna, Austria). The stack of images was reconstructed to a three-dimension visualization model in 3D Slicer software (a free, open-source platform; http://www.slicer.org).

Thickness measurement of the medial wall of the CS

The thickness of the sellar part medial wall of the CS was measured in 12 sets (24 sides, 10 sides in axial, and 14 sides in coronal plane) of the ultra-thin plastinated section using TissueFAXS Imaging Software (TissueGnostics, Vienna, Austria). From each set of sections, 6 sections were selected for the measurement on average. On the coronal sections, the thickness of the sellar part medial wall at point C1–C6 was measured from superior to inferior (Fig. 1a). Similarly, the thickness at point H1–H6 was measured from anterior to posterior on the horizontal sections (Fig. 1b). Therefore, the thickness measurement was performed at 36 points in each sellar part medial wall. The Mann–Whitney *U* test was used to compare the thickness of the sellar part medial wall at nine different regions (anterior–superior, mid-superior, posterior-superior, mid-anterior, central, mid-posterior, anterior-inferior, mid-inferior, and posterior-inferior) (Fig. 3a). $P < 0.05$ was considered a statistically significant difference.

Results

The sellar part medial wall is an intact dural layer

The CS has a recognizable sellar part medial wall that separates the CS from the pituitary gland. On its lateral surface, there were varying amounts of loose connective tissue. However, in most cases, these loose connective tissues were intermittent, or they were continuous only on a certain section. Only in a few cases, they formed a complete layer of structure (Figs. 1 and 5). Superiorly, this wall adhered to the diaphragma sellae to form a fibrous triangle. Although there were venous channels within it, this superior fibrous triangle was constant (Fig. 1c). At its anterior, posterior, and inferior border, the sellar part medial wall fused with the periosteal dura of the sella turcica to form the anterior, posterior, and inferior fibrous triangles, respectively (Fig. 1d–f). However, these three fibrous triangles were disrupted frequently by intercavernous sinuses (Fig. 1f–h).

In 5 of 12 specimens (24 sides), 8 micro-protrusions of the pituitary gland were found at both sides of the sellar part medial wall (Fig. 2; Table 1). These protrusions can be classified in two different profiles: cone-shaped (5 cases) and nipple-shaped (3 cases). The adenohypophysis protrusions accounted for 6 cases of the hernial content, while the neurohypophysis protrusions accounted for the other 2 cases. Five out of 6 adenohypophysis protrusions were identified at the mid-inferior portion of the sellar part medial wall, protruding into the inferior fibrous triangle (Fig. 2a, b, f–h). The two neurohypophysis protrusions were found at the posterior-superior portion of the sellar part medial wall (Fig. 2c, e). The mean diameter at the mouth of the hernial sac was 0.76 ± 0.52 mm (0.29 ~ 1.79 mm). The dural covering of these protrusions became loose and thinner than the neighboring medial wall.

Thickness measurement of the sellar part medial wall

The thickness of the sellar part medial wall was measured and compared at nine different regions (36 points), and the mean thicknesses were shown in Table 2. The thickness of the sellar part medial wall at the central portion (42.92 ± 16.01 μm) was significantly thinner than that at the other 8 surrounding portions (Fig. 3; Table 2). The thickness of the sellar part medial wall at the posterior-inferior portion in the left side (66.85 ± 40.17 μm) was thinner than that in the right side (89.08 ± 54.54 μm, $P < 0.05$) (Table 2).

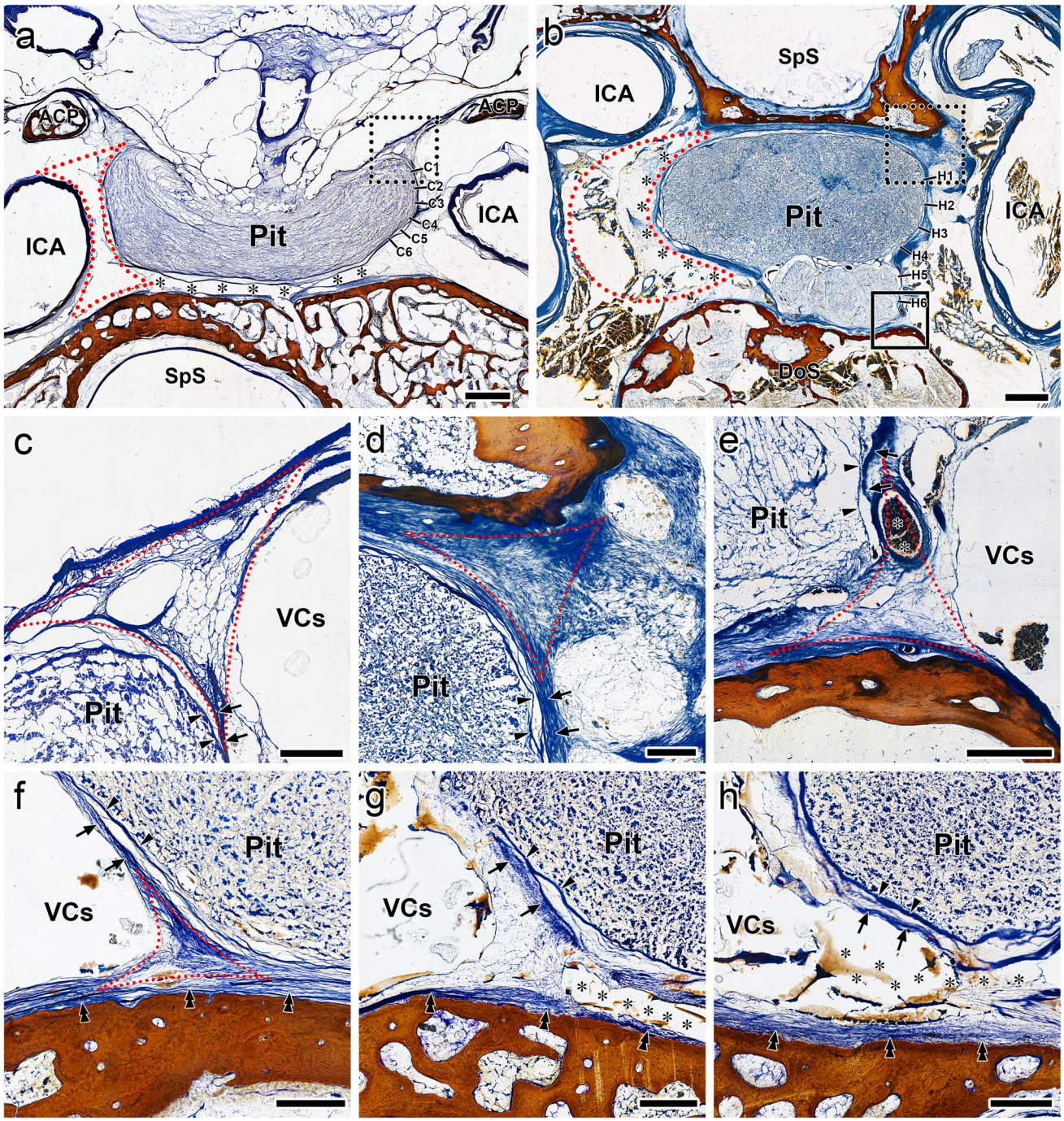

Fig. 1 **a** Overview coronal section through the pituitary stalk. There was a double-concave space (red dotted line area) between the inward bending ICA and the sellar part medial wall. The C1–C6 indicate thickness measurement points on each sellar part medial wall in coronal sections. The intercavernous sinus (asterisks) interconnected the right and the left CS at the sellar floor. **b** Overview axial section through the central part of the pituitary gland. A crescent-shaped space (red dotted line area) was located between the outward bending ICA and the sellar part medial wall. The H1–H6 indicate thickness measurement points on axial sections. A continuous layer of loose connective tissues (asterisks) lined on the lateral surface of the left sellar part medial wall in this case. **c**–**e** Enlarged view of the dotted line box in panels **a** and **b** and the solid line box in panel **b**, respectively, showing the superior, anterior, and posterior fibrous triangles (red dotted line area). Note that a small artery (asterisks) was passing through the medial wall in panel **e**. **f**–**h** Serial coronal sections showing the inferior fibrous triangle (red dotted line area) interrupted by the intercavernous sinus (asterisks). Arrows indicate the sellar part medial wall, arrowheads indicate the capsule of the pituitary gland, and double arrowheads indicate the periosteum of the sphenoid bone. ACP, anterior clinoid process; DoS, dorsum sellae; ICA, internal carotid artery; Pit, pituitary gland; SpS, sphenoid sinus; VCs, venous channels. Bars = 2 mm in panels **a** and **b**; bars = 500 μm in panels **c**–**h**

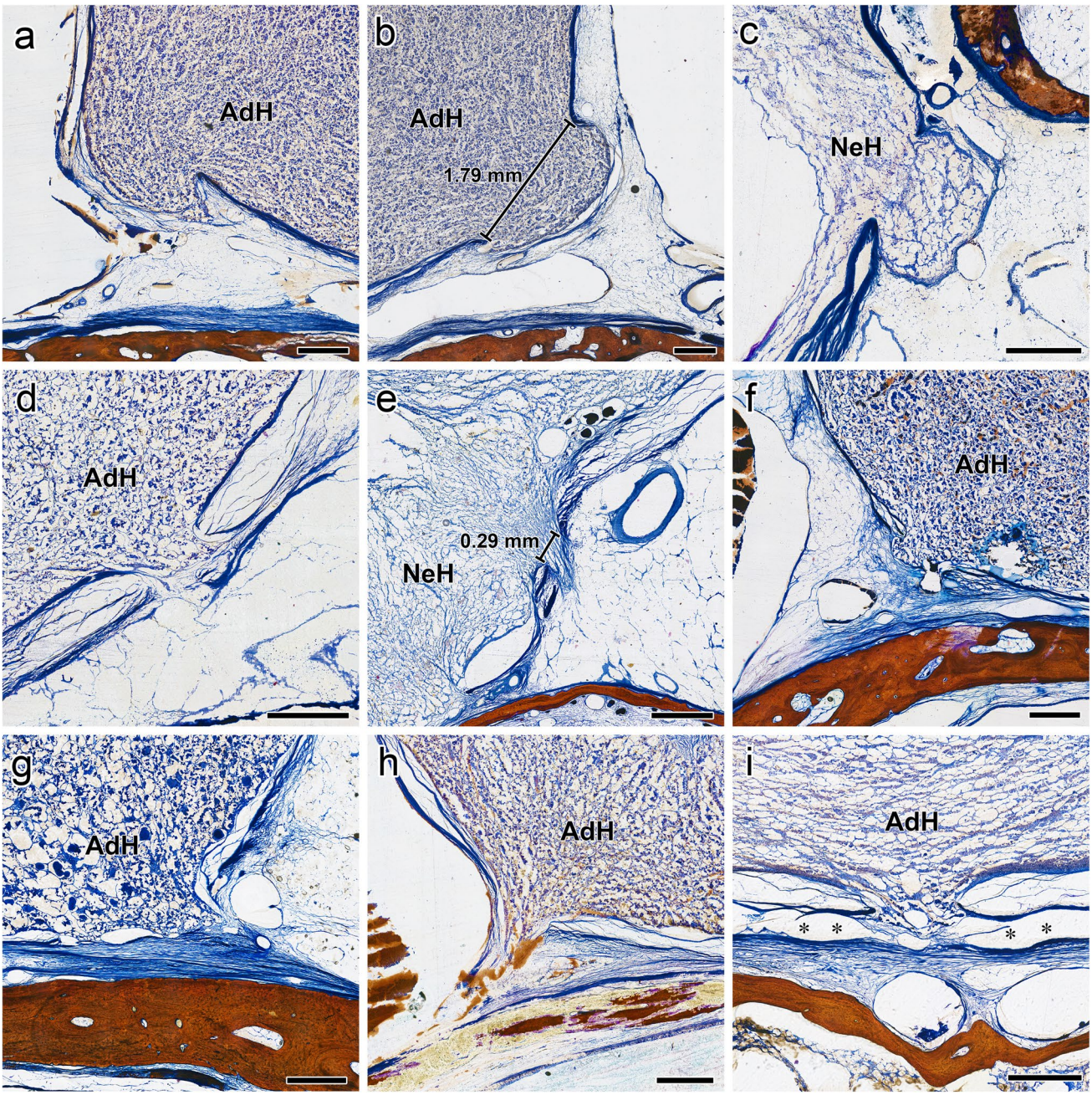

Fig. 2 **a**–**h** The different types of micro protrusions of the pituitary gland shown in Table 1. Panels **a**–**c** and **f**–**h** are in coronal sections, and panels **d** and **e** are in axial sections. The maximum (1.79 mm) and minimum (0.29 mm) diameters of the mouth of the hernial sac were shown in panels **b** and **e**, respectively. (**i**) Another coronal section showing a micro protrusion of the pituitary gland protruding into the intercavernous sinus (asterisks) in the sellar floor. AdH, adenohypophysis; NeH, neurohypophysis. Bars = 500 µm

Relationships between the ICA and the sellar part medial wall

The relationship between the intracavernous carotid and the sellar part medial wall was examined at the 3-dimensional reconstruction model based on the serial ultra-thin plastinated sections. From the lateral view, 20 of 24 sides (83.3%) of intracavernous carotid arteries coursed above the level of the sellar floor and covered more than the inferior one-third of the sellar part medial wall, which were classified as the supra sellar floor type ICA (Fig. 4a). In the remaining 4 cases (16.7%), these intracavernous carotid arteries covered less than the inferior one-third of the wall in 3 sides, and coursed below the level of the sellar floor in 1 side. In the 20 cases of the supra sellar floor

Table 1 Micro-protrusions of the pituitary gland in the sellar part medial wall

Specimen number	Side	Location in the sellar part medial wall	Protrusion type	Shape	Diameter at the mouth of the hernial sac	Panel in Fig. 2
P1	Left	Mid-inferior	Adenohypophysis	Cone-shaped	1.34 mm	a
	Right	Mid-inferior	Adenohypophysis	Nipple-shaped	1.79 mm	b
	Right	Posterior-superior	Neurohypophysis	Nipple-shaped	0.62 mm	c
P2	Right	Central	Adenohypophysis	Cone-shaped	0.45 mm	d
	Right	Posterior-superior	Neurohypophysis	Cone-shaped	0.29 mm	e
P3	Left	Mid-inferior	Adenohypophysis	Nipple-shaped	0.51 mm	f
P4	Right	Mid-inferior	Adenohypophysis	Cone-shaped	0.49 mm	g
P5	Left	Mid-inferior	Adenohypophysis	Cone-shaped	0.56 mm	h

Table 2 Thickness measurement of the sellar part medial wall of the CS in nine regions

	Anterior superior	Mid-superior	Posterior superior	Mid-anterior	Central	Mid-posterior	Anterior inferior	Mid-inferior	Posterior inferior
Left	63.28 ± 29.75	52.03 ± 31.82	60.98 ± 40.76	50.14 ± 20.46	41.98 ± 12.34*	50.07 ± 23.38	65.47 ± 32.89	67.43 ± 46.22	66.85 ± 40.17
Right	66.54 ± 44.47	50.17 ± 24.87	58.45 ± 29.53	55.33 ± 21.53	43.87 ± 19.10*	61.39 ± 43.79	70.51 ± 43.61	70.12 ± 50.84	89.08 ± 54.54
Total	64.91 ± 30.17	51.10 ± 28.43	59.71 ± 35.87	52.73 ± 21.04	42.92 ± 16.01*	55.73 ± 35.35	67.99 ± 42.81	68.78 ± 48.35	77.96 ± 48.94

All thickness measurements expressed in microns (μm) and presented as mean ± SD. Results are listed for the left side, right side, and the total

*$P < 0.05$ for comparisons of group means (Mann–Whitney U test)

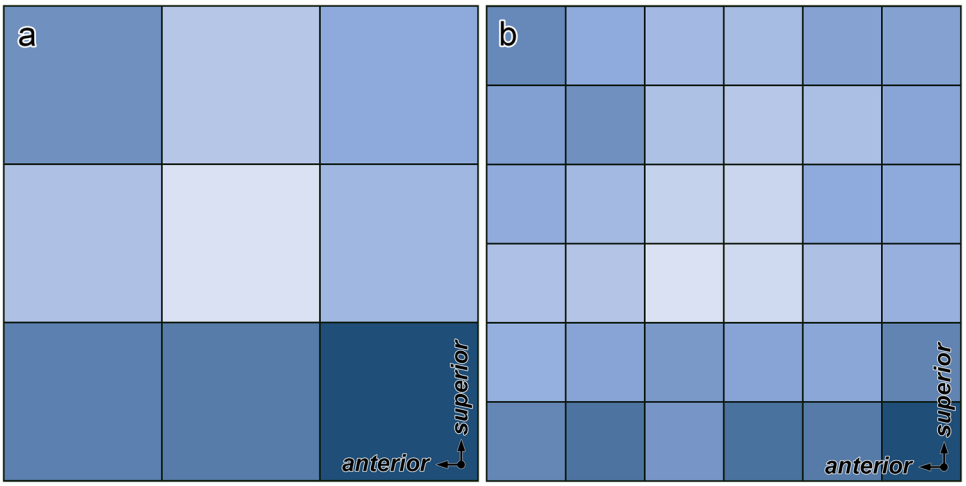

Fig. 3 The nine-region (**a**) and 36 points (**b**) heat map of the thickness of the sellar part medial wall based on Table 2

type ICA, according to the boundary line from its posterior vertical segment to its anterior vertical segment, these intracavernous carotid arteries bent towards the sellar part medial wall in 13 sides (65%) and bent outward in 7 sides (35%) (Fig. 4b). Whereas in the remaining 4 cases of the infra sellar floor type ICA, all those intracavernous carotid arteries bent outward.

There was a crescent-shaped space between the outward bending type ICA and the medial wall, whereas there was a double-concave medial CS compartment when the intracavernous carotid bent inward (Fig. 1a, b). The minimum distance between the intracavernous carotid and the sellar part medial wall was 0.59 ± 0.43 mm when the intracavernous carotid bent inward. In 11 out of 13 cases (84.6%) of the inward bending ICA, those projective points of the minimum distance were located at the central part of the sellar part medial wall (Fig. 4c). In transparent plastinated slices of 2 specimens, the excessive inward bending of the intracavernous carotid squeezed the central portion of the sellar part medial wall and the pituitary gland, with the result that the pituitary gland protruded to 4 fibrous triangles at the edge of that wall (Fig. 4d, e).

Configuration of the medial compartment of the CS

Due to its position and bending pattern, the intracavernous carotid had a changeable relationship with the sellar part medial wall, and, as a result, the medial compartment of the CS between

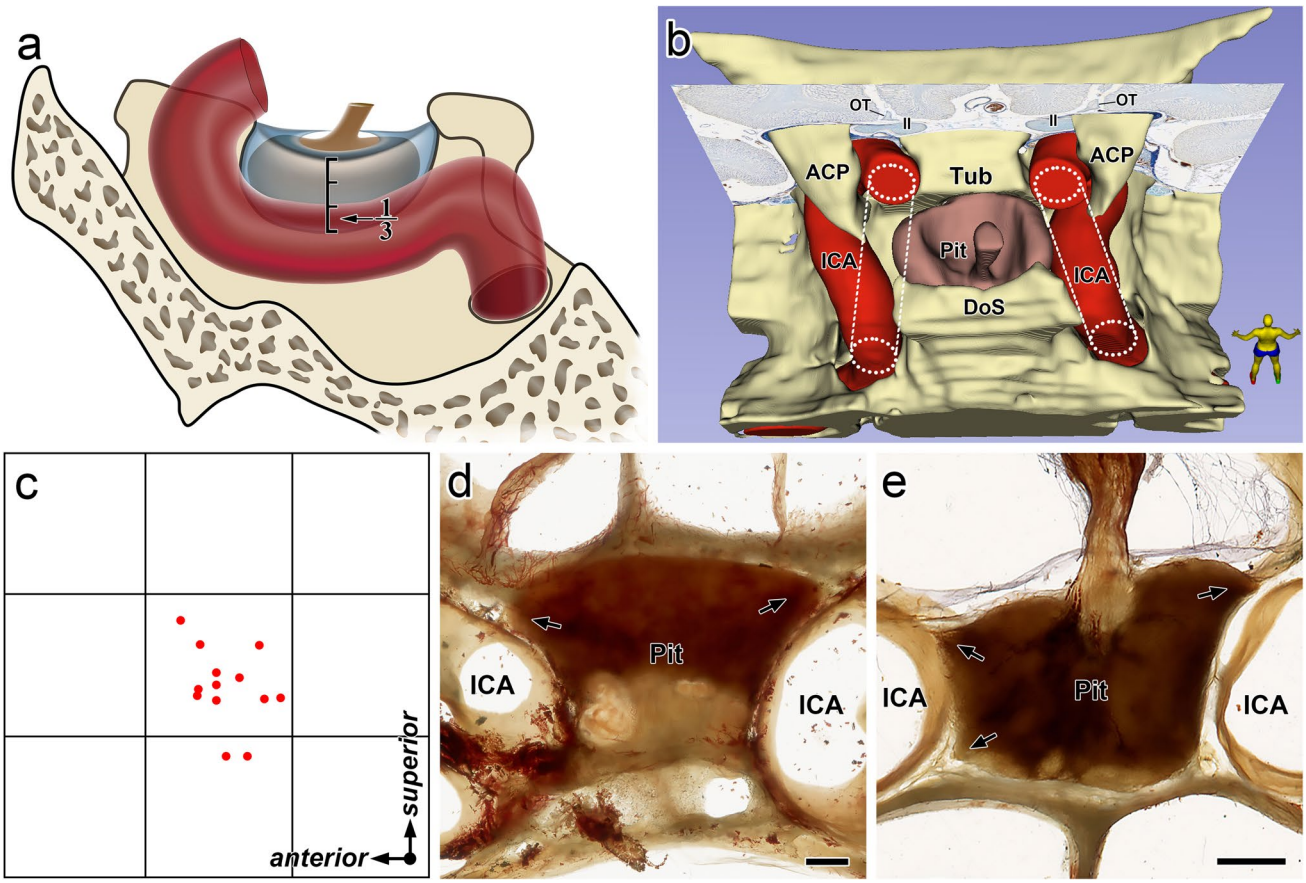

Fig. 4 **a** Diagram of the lateral view of the CS showing the relationship between the intracavernous carotid and the sellar part medial wall. The intracavernous carotid covered more than the inferior one-third of that wall, which was classified as the supra sellar floor type ICA. The artery covered less than the inferior one-third or coursed below the level of the sellar floor was classified as the infra sellar floor type. **b** The 3-dimensional visualization model reconstructed based on a set of coronal ultra-thin plastination sections showing the different bending facing states of tortuous intracavernous carotid arteries from the superior view. According to the boundary line (parallel dashed line) from its posterior vertical segment to its anterior vertical segment, the intracavernous carotid arteries were divided into outward bending type (left side) and inward bending type (right side). **c** Scatter diagram showing, on the sellar part medial wall, projective points of the shortest distance between the inward bending ICA and that wall. Axial (**d**) and coronal (**e**) transparent plastination slices showing tongue-like protrusions of the pituitary (arrows) caused by excessive compression of the inward bending ICA. ACP, anterior clinoid process; DoS, dorsum sellae; ICA, internal carotid artery; II, optic nerve; OT, olfactory tract; Pit, pituitary gland; Tub, Tuberculum sellae. Bars = 2 mm

them varied markedly. When the intracavernous carotid bent outward or coursed below the level of the sellar floor, the medial compartment of the CS was apt to form a wider space (Figs. 1b, 4b, and 5). In contrast, the medial compartment could be partially or completely occupied by the inward bending of the intracavernous carotid (Figs. 1a, 4b, and 5).

Macroscopically, in addition to venous channels and arteries, there were several fibrous bands in the medial compartment of the CS. Generally, the closer the distance between the ICA and the sellar part medial wall, the wider and shorter the fibrous bands (Fig. 5). Histologically, the caroticoclinoid ligament, which connected the anterior clinoid process and the sellar part medial wall, was the constant dense regular connective tissue ligamentous structure among these fibrous bands (Fig. 5c–e). This dense connective caroticoclinoid ligament was identified in 21 of 24 sides (87.5%) at the serial ultra-thin plastinated sections. Except for the caroticoclinoid ligament, the other fibrous bands were almost the loose connective tissue connections, which were mainly composed of the adipose tissue sandwiched between two layers of the vascular endothelium of venous channels (Fig. 5a, b, f, g). When the ICA was close to the sellar part medial wall, it was found that there were more densely stained connective tissues in these fibrous bands (Fig. 5f).

Discussion

The medial wall of the CS has a significant role in evaluation and treatment of pituitary adenomas. There are many microsurgical, histological, and radiologic studies on the medial

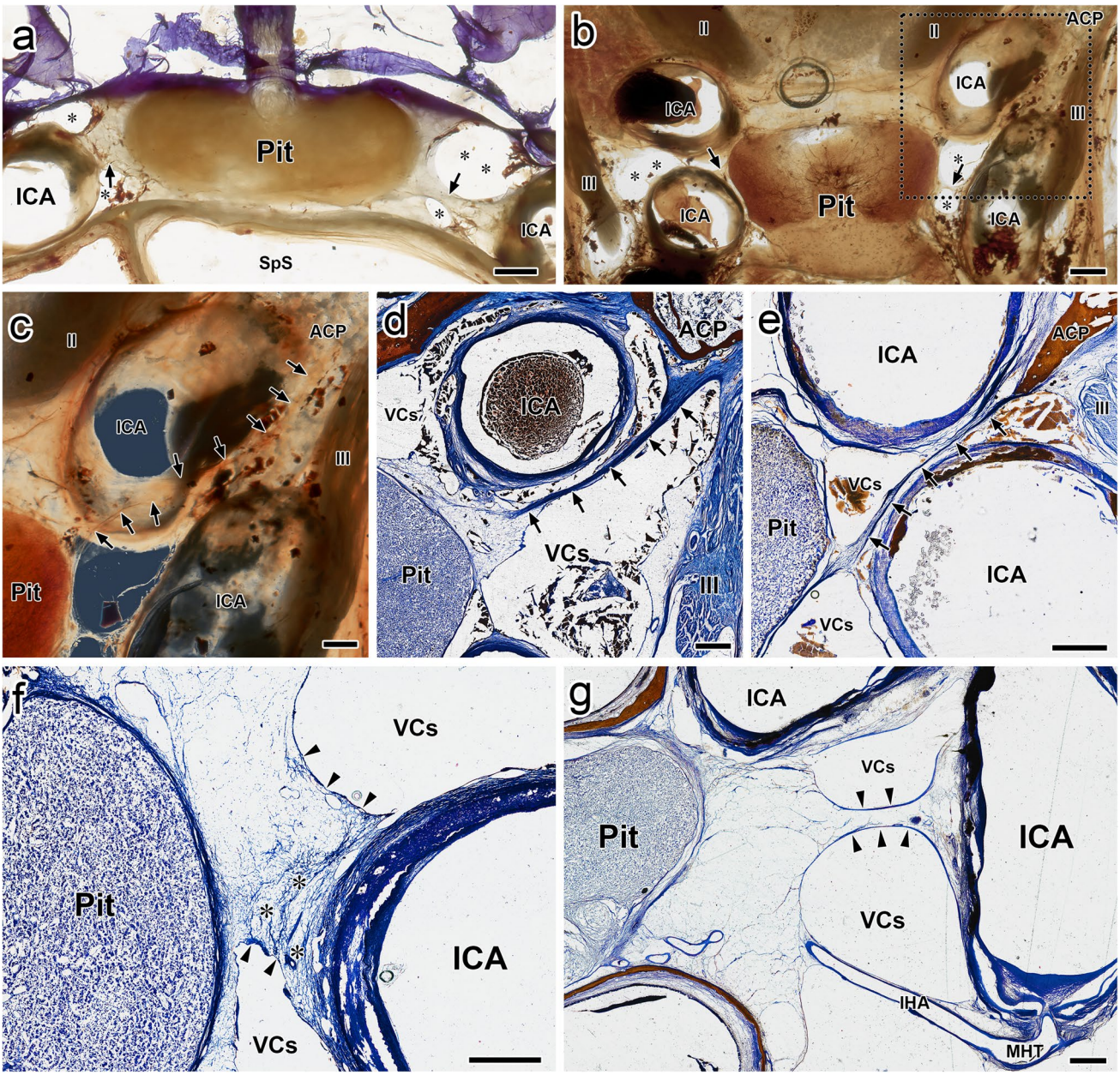

Fig. 5 Coronal (**a**) and axial (**b**) transparent plastination slices showing the configuration of the medial compartment of the CS. There were fibrous bands (arrows) connected between the intracavernous carotid and the sellar part medial wall, which varied in length, width and thickness. Asterisks indicate venous channels of the CS. **c** Enlarged view of the dotted line box in panel **b**, showing the caroticoclinoid ligament (arrows) connected the anterior clinoid process and the medial wall. Axial (**d**) and coronal (**e**) sections showing the caroticoclinoid ligament (arrows) is the dense regular connective tissue ligamentous structure. Note that there was no loose connective tissues layer lined on the lateral surface of the sellar part medial wall in that section in panel **e**. Coronal (**f**) and axial (**g**) sections showing different types of fibrous bands. These fibrous bands were formed by adipose tissue wrapped by endothelium of venous channels (arrowheads). When the ICA was close to the sellar part medial wall, it was found that there were more densely stained connective tissues in these fibrous bands (asterisks in panel **f**). Note that the meningohypophyseal trunk, which arises from the posterior bend of the intracavernous carotid, gave off the inferior hypophyseal artery, running through the medial CS compartment. ACP, anterior clinoid process; ICA, internal carotid artery; IHA, inferior hypophyseal artery; II, optic nerve; III, oculomotor nerve; MHT, meningohypophyseal trunk; Pit, pituitary gland; SpS, sphenoid sinus; VCs, venous channels. Bars = 2 mm in panels **a** and **b**, bars = 1 mm in panels **c**–**g**

wall of the CS [1, 7, 11–25], but technically, it is still a challenge to identify this delicate meningeal layer structure at the skull base. In this study, the fine architecture of the medial wall and medial compartment of the CS were investigated at both macro- and micro-levels by using the epoxy sheet plastination technique.

Most studies believed that the medial wall of the CS was formed by the dural layer [1, 5, 7, 11, 12, 16, 21, 23, 26], which was also considered to be an anatomical weak point of the CS. According to Yasuda et al. [5], the dural medial wall of the CS was divided into two parts: the sellar and the sphenoidal. The sellar part is a dural membrane that separates the pituitary fossa from the CS, and the sphenoidal part covers the lateral surface of the body of the sphenoid bone [1, 5]. The sphenoidal part was also recommended to be identified as the anterior wall of the CS under the endonasal endoscopic approach [7]. Nevertheless, a few previous studies suggested that there was no a dural medial wall, and the only dense connective layer separating the pituitary from the CS was the capsule of the pituitary gland [14, 17, 22, 24]. But in the work of Ceylan et al. [11], the pituitary capsule and the medial wall were identified as two different structures by examining the expression levels of collagenous proteins. In this study, by using serial large plastinated sections, we focused on the sellar part medial wall of the CS, which was a distinct single dural layer. Although they were close together, the dural medial wall and the capsule of the pituitary gland were easy to distinguish in most cases. On the lateral surface of sellar part medial wall, there were varying amounts of loose connective tissue. In a few specimens, these loose connective tissues formed a complete layer of structure, which was ever defined as the inner fibrous layer of the medial wall by Songtao et al. [22]. While in most cases, these loose connective tissues were scattered, or only formed a continuous structure on a certain section. However, this loose circumferential fibrous bed was considered to be the main factor to explain the high incidence of extension of pituitary tumors to the CS [14].

The pituitary adenomas could easily extend into the CS due to anatomical weaknesses or fenestrations in the medial wall of the CS [24, 27, 28]. The medial wall separates venous channels in the CS from the pituitary fossa. If there is a perforation in the medial wall, the blood in venous channels could enter the pituitary fossa. Indeed, it is true that the intercavernous sinus drain into the pituitary fossa via the perforation on the medial wall. Nevertheless, the intercavernous sinus only passed between the meningeal dural sellar part medial wall and the periosteal dura of the sella turcica, and there was no perforation on the sellar part medial wall itself. In this study, we observed the sellar part medial wall fused with the periosteal dura of the sella turcica to form the fibrous triangle at its anterior, posterior and inferior border. Furthermore, these fibrous triangles often splitted for the passage of the intercavernous sinus. Although they did not perforate on the sellar part medial wall, these intercavernous sinuses provided potential space for tumor growth from the sella to the CS and vice versa [27, 28].

In another study, Yokoyama et al. found small histological defects on the medial wall in 3 of 30 coronal sections, and the authors suggested that those defects were important with regard to the extension of adenomas [24]. Conversely, in subsequent anatomical, histological, and diaphanoscopic studies, they did not find such defects in the medial wall of the CS [5, 18, 20, 23]. In our study, we observed 8 similar micro protrusions of the pituitary gland bulging toward the CS in the sellar part medial wall in 5 of 12 specimens (41.7%). In addition, there was another case of pituitary protrusion protruding into the intercavernous sinus in the sellar floor (Fig. 2i). These protrusions originated from both adenohypophysis and neurohypophysis, and were conical and papillary in shape. Nevertheless, there were no obvious gaps on the hernial sac, but only the dural covering of these protrusions became loose and thinner than the neighboring medial wall.

Although it is unclear how these protrusions are formed, we believe they could play a role in tumor invasion and residual tumor recurrence. Despite there was an intact dural medial wall, these protrusions were likely to be anatomical weak points on it. Interestingly, however, we found that 5 out of 6 adenohypophysis protrusions protruded into the relatively stronger inferior fibrous triangle at the mid-inferior portion of the sellar part medial wall, rather than the thinner central portion of that wall. The growth of tumor tissue could extend into the inferior CS compartment via this route and eventually develop into the Grade 3B adenomas. It was reported that the preferential inferior extension of tumor was seen mostly in growth hormone-secreting adenomas [29–31].

On the other hand, if there are very small microadenomas developed in these micro protrusions, such microscopic dural invasion is difficult to be detected during surgery. Moreover, because the protrusion was often trapped in the hernia dural sac, it might be very difficult to remove surgically, which would provide an opportunity for the recurrence of residual tumor. In a recent study, Nagata et al. found 4 (57.1%) occult medial wall invasions among the 7 patients without intraoperative apparent medial wall involvement [9]. Similarly, in another study, it was reported that there were two of three patients with Knosp Grade 0 and without any evidence of the medial wall invasion had microscopic disease on their histopathologic analyses [10]. The unrecognized occult dural invasion could be an important cause of surgical failure [10, 32]. Therefore, considering the recurrence of residual tumors, it was recommended to remove the medial wall of the CS after adenomectomy, especially in patients with functional adenomas [9, 10]. Several groups have recently shown that it is safe and feasible to remove the medial wall of the CS when performed by experienced neurosurgeons [6, 7, 9, 10].

The key factor that determines the parasellar tumor extension is the resistance of the structure of the medial wall of the CS [18, 20, 21]. Thickness measurements of the medial wall are helpful to examine anatomical weak areas with

low resistance. There have been many quantitative studies on the medial wall, but the thickness of the wall varied between them [20–24], which may be due to the different locations and number of measurement points selected. In this study, thickness measurements were made at 36 points evenly distributed on each sellar part medial wall. According to the data, it was shown on the nine-region thickness heat map that the central portion of the sellar part medial wall (42.92 ± 16.01 μm) was significantly thinner than the other 8 surrounding portions. This finding was consistent with a previous diaphanoscopic study [18], which suggested the weakest area of the sellar part medial wall was slightly anterior to its center in 13 out of 14 specimens. Consequently, if only considering its anatomical nature, the central portion of the sellar part medial wall is the weakest area for tumor extension.

Furthermore, at the lateral aspect of the medial wall, the structures within the CS may also affect the direction of growth of pituitary adenomas. The intracavernous carotid, an important landmark used for the imaging classification of CS invasions [30, 33], has a close spatial relationship with the medial wall. The medial CS compartment is located between the intracavernous carotid and the medial wall. The tortuous intracavernous carotid was usually studied from lateral view [5, 34, 35], which was divided into five parts: the posterior vertical segment, the posterior bend, the horizontal segment, the anterior bend, and the anterior vertical segment. Nevertheless, few reports investigated it from the superior view [35]. In this study, 24 intracavernous carotid arteries were classified into two categories: supra sellar floor type (20 cases) and infra sellar floor type (4 cases). The supra sellar floor type ICA was considered to be closely related to the sellar part medial wall, which coursed above and covered more than the inferior one-third of the sellar part medial wall. In 13 out of 20 cases of the supra sellar floor type ICA, these intracavernous carotid arteries bent towards the sellar part medial wall, with the result that the medial CS compartment was compressed into a double-concave space. While in the remaining 7 cases of the supra sellar floor type ICA and all 4 infra sellar floor type ICAs, accounting for 45.8% of the total 24 sides, these arteries bent outward and made an ample crescent-shaped medial venous space. These findings were in accordance with results of 48% the medial venous space dominant in 50 cases reported by Inoue et al. [35].

Therefore, it can be assumed that when the intracavernous carotid bends outward or the artery courses below the level of the sellar floor, there will be an adequate medial venous space for the growing pituitary tumor to push the sellar part medial wall outward, and the tumor is most likely to invade into the CS through the weakest central part of this wall (Fig. 6). On the contrary, when the intracavernous carotid bends to the sellar part medial wall, the medial CS compartment frequently occupied by the tortuous artery and even absent. If the intracavernous carotid compresses the sellar part medial wall and the pituitary gland excessively, this will result in tongue-like protrusions of the pituitary gland extending around the artery [5, 12], which can also be seen on our transparent plastinated slices. The development of an adenoma on these tongue-like protrusions could easily mimic the CS invasion [12]. It is noteworthy that in 11 out of 13 cases (84.6%) of the inward bending intracavernous carotid, we found that the location of the minimum distance between the artery and the medial wall was projected on the central part of the sellar part medial wall. In addition, when the intracavernous carotid was close to the sellar part medial wall, there were usually wide and short fibrous bands with more densely stained connective tissues, which were

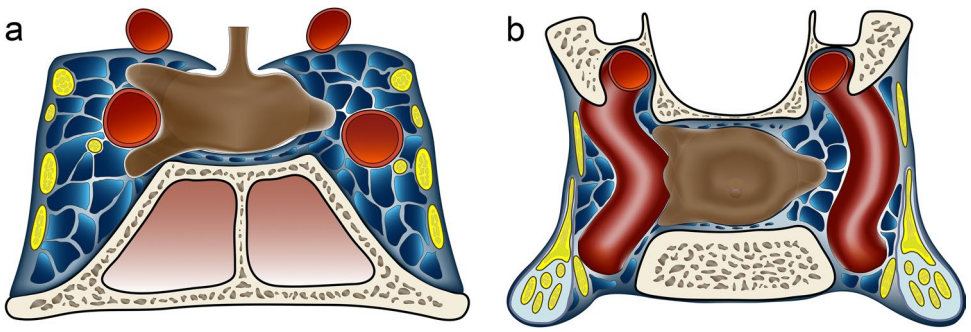

Fig. 6 Schematic drawing of the coronal (**a**) and axial (**b**) view of the sella turcica and the CS, illustrating the possible tumor extension pathways based on anatomical nature of the sellar part medial wall and the bending facing state of the tortuous intracavernous carotid. When the intracavernous carotid bends outward or the artery courses below the level of the sellar floor (right side), there will be an adequate medial venous space for the growing pituitary tumor to push the sellar part medial wall outward, and the tumor is most likely to invade into the CS through the weakest central part of this wall. On the contrary, when the intracavernous carotid bends to the sellar part medial wall (left side), the weakest central part of the sellar part medial wall could be enhanced by the combined patch of these fibrous bands, the adventitia, and the arterial wall, and then the growing tumor is more likely to enter other CS compartments directly through the periphery of the medial wall

connected between the artery and the wall. In this instance, the parasellar extension of the pituitary tumor will push the medial wall to cover the intracavernous carotid. At this time, the weakest central part of the sellar part medial wall could be enhanced by the combined patch of these fibrous bands, the adventitia, and the arterial wall, and then, the growing tumor is more likely to enter other CS compartments directly through the periphery of the medial wall (Fig. 6). Still, if the dural medial wall plus the patch layer structures are enough to resist the tumor growth, suprasellar extension may be another option.

These fibrous bands in the medial CS compartment have been mentioned in several previous reports [7, 9, 11, 36, 37] and were considered to have important clinical significance in the transcavernous approach [7]. Truong et al. [7] classified these ligamentous dura-like trabeculae into 4 groups based on their trajectory. However, in our study, the caroticoclinoid ligament was the only fibrous band that we could consistently identify as a dense regular connective tissue ligamentous structure, which connected the anterior clinoid process to the medial wall. Other fibrous bands, although they looked like ligaments macroscopically, were actually formed by adipose tissue wrapped by endothelium of venous channels, which could be cut easily by a blunt-tipped dissector [9]. Although these fibrous bands had different properties, they were still important landmarks during surgery.

Limitation of the study

This study described the fine architecture of the medial wall and medial compartment of the CS and discussed the tumor extension pathways based on their anatomical nature. However, the factors that determine the direction of growth of pituitary adenomas, such as the origin and biological behavior of tumors, cannot be ignored. The relatively small sample size and elderly specimens are the other limitations of the present study. As the arteries gradually elongate and bend with age, the tortuous intracavernous carotid in elderly specimens showed a more obvious trend of bending inward or outward, and there was a lack of intermediate type.

Conclusions

This study provided a precise description of the fine architecture of the medial wall and medial compartment of the CS. The micro-pituitary protrusion in the sellar part medial wall could provide a potential opportunity for the occult tumor invasion and the recurrence of residual tumor. The tortuous intracavernous carotid bent inward or outward may be a factor of the determination of the direction of growth of pituitary adenomas.

Acknowledgements The authors sincerely thank those who donated their bodies to science so that anatomical research could be performed.

Author contribution All authors contributed to the study conception and design. Material preparation, data collection, and analysis were performed by Kaili Shi, Zhifan Li, Chunjing Ma, Xingyu Zhu, and Liu Xu. The first draft of the manuscript was written by Kaili Shi and Liang Liang, and all authors commented on previous versions of the manuscript. All authors read and approved the final manuscript.

Funding This work was supported by the Natural Science Foundation of the Anhui Higher Education Institutions of China (No. KJ2020A0145) and the National Natural Science Foundation of China (No. 31500967).

Data availability Not applicable.

Declarations

Ethical approval This study was performed in line with the principles of the Declaration of Helsinki. This study was approved by the Ethics Committee of Anhui Medical University.

Consent to participate Not applicable.

Human and animal ethics Not applicable.

Consent for publication Not applicable.

Competing interests The authors declare no competing interests.

References

1. Campero A, Campero AA, Martins C, Yasuda A, Rhoton AL Jr (2010) Surgical anatomy of the dural walls of the cavernous sinus. J Clin Neurosci 17:746–750. https://doi.org/10.1016/j.jocn.2009.10.015
2. Rhoton AL Jr (2002) The cavernous sinus, the cavernous venous plexus, and the carotid collar. Neurosurgery 51:S375-410
3. Yasuda A, Campero A, Martins C, Rhoton AL Jr, de Oliveira E, Ribas GC (2005) Microsurgical anatomy and approaches to the cavernous sinus. Neurosurgery 56:4–27 discussion 24–27
4. Chung BS, Chung MS, Park JS (2015) Six walls of the cavernous sinus identified by sectioned images and three-dimensional models: anatomic report. World Neurosurg 84:337–344. https://doi.org/10.1016/j.wneu.2015.03.049
5. Yasuda A, Campero A, Martins C, Rhoton AL Jr, Ribas GC (2004) The medial wall of the cavernous sinus: microsurgical anatomy. Neurosurgery 55:179–189 discussion 189–190
6. Cohen-Cohen S, Gardner PA, Alves-Belo JT, Truong HQ, Snyderman CH, Wang EW, Fernandez-Miranda JC (2018) The medial wall of the cavernous sinus. Part 2: selective medial wall resection in 50 pituitary adenoma patients. J Neurosurg 131:131–140. https://doi.org/10.3171/2018.5.Jns18595
7. Truong HQ, Lieber S, Najera E, Alves-Belo JT, Gardner PA, Fernandez-Miranda JC (2018) The medial wall of the cavernous sinus. Part 1: surgical anatomy, ligaments, and surgical technique for its mobilization and/or resection. J Neurosurg 131:122–130. https://doi.org/10.3171/2018.3.JNS18596
8. Goel A (2016) Letter to the Editor: Pituitary tumors and cavernous sinus extension. J Neurosurg 124:1129–1130. https://doi.org/10.3171/2015.5.Jns151148

9. Nagata Y, Takeuchi K, Yamamoto T, Ishikawa T, Kawabata T, Shimoyama Y, Wakabayashi T (2019) Removal of the medial wall of the cavernous sinus for functional pituitary adenomas: a technical report and pathologic significance. World Neurosurg 126:53–58. https://doi.org/10.1016/j.wneu.2019.02.134
10. Omar AT, Munoz DG, Goguen J, Lee JM, Rotondo F, Kovacs K, Cusimano MD (2020) Resection of the medial wall of the cavernous sinus in functioning pituitary adenomas: Technical note and outcomes in a matched-cohort study. Clin Neurol Neurosurg 106306. https://doi.org/10.1016/j.clineuro.2020.106306
11. Ceylan S, Anik I, Koc K, Kokturk S, Ceylan S, Cine N, Savli H, Sirin G, Sam B, Gazioglu N (2011) Microsurgical anatomy of membranous layers of the pituitary gland and the expression of extracellular matrix collagenous proteins. Acta Neurochirurgica 153:2435–2443. https://doi.org/10.1007/s00701-011-1182-3discussion 2443
12. Destrieux C, Kakou MK, Velut S, Lefrancq T, Jan M (1998) Microanatomy of the hypophyseal fossa boundaries. J Neurosurg 88:743–752
13. Diao Y, Liang L, Yu C, Zhang M (2013) Is there an identifiable intact medial wall of the cavernous sinus? Macro- and microscopic anatomical study using sheet plastination. Neurosurgery 73:ons106-109. https://doi.org/10.1227/NEU.0b013e3182889f2b discussion ons110
14. Dietemann JL, Kehrli P, Maillot C, Diniz R, Reis M Jr, Neugroschl C, Vinclair L (1998) Is there a dural wall between the cavernous sinus and the pituitary fossa? Anatomical and MRI findings. Neuroradiology 40:627–630
15. Goncalves MB, de Oliveira JG, Williams HA, Alvarenga RM, Landeiro JA (2012) Cavernous sinus medial wall: dural or fibrous layer? Systematic review of the literature. Neurosurg Rev 35:147–153. https://doi.org/10.1007/s10143-011-0360-3 discussion 153–144
16. Kawase T, van Loveren H, Keller JT, Tew JM (1996) Meningeal architecture of the cavernous sinus: clinical and surgical implications. Neurosurgery 39:527–534 discussion 534–526
17. Kehrli P, Ali M, Reis M Jr, Maillot C, Dietemann JL, Dujovny M, Ausman JI (1998) Anatomy and embryology of the lateral sellar compartment (cavernous sinus) medial wall. Neurol Res 20:585–592
18. Knappe UJ, Konerding MA, Schoenmayr R (2009) Medial wall of the cavernous sinus: microanatomical diaphanoscopic and episcopic investigation. Acta neurochirurgica 151:961–967. https://doi.org/10.1007/s00701-009-0340-3 discussion 967
19. Kural C, Simsek GG, Guresci S, Arslan E, Kilic C, Tehli O, Geyik M, Erbas C, Izci Y (2015) Histological structure of the medial and lateral walls of cavernous sinus in human fetuses. Child's Nerv Syst 31:699–703. https://doi.org/10.1007/s00381-015-2644-3
20. Kursat E, Yilmazlar S, Aker S, Aksoy K, Oygucu H (2008) Comparison of lateral and superior walls of the pituitary fossa with clinical emphasis on pituitary adenoma extension: cadaveric-anatomic study. Neurosurg Rev 31:91–98. https://doi.org/10.1007/s10143-007-0112-6 discussion 98–99
21. Peker S, Kurtkaya-Yapicier O, Kilic T, Pamir MN (2005) Microsurgical anatomy of the lateral walls of the pituitary fossa. Acta Neurochirurgica 147:641–648. https://doi.org/10.1007/s00701-005-0513-7 discussion 649
22. Songtao Q, Yuntao L, Jun P, Chuanping H, Xiaofeng S (2009) Membranous layers of the pituitary gland: histological anatomic study and related clinical issues. Neurosurgery 64:ons1-9. https://doi.org/10.1227/01.NEU.0000327688.76833.F7 discussion ons9–10
23. Yilmazlar S, Kocaeli H, Aydiner F, Korfali E (2005) Medial portion of the cavernous sinus: quantitative analysis of the medial wall. Clin Anat 18:416–422. https://doi.org/10.1002/ca.20160
24. Yokoyama S, Hirano H, Moroki K, Goto M, Imamura S, Kuratsu JI (2001) Are nonfunctioning pituitary adenomas extending into the cavernous sinus aggressive and/or invasive? Neurosurgery 49:857–862 discussion 862–853
25. Yasuda A, Campero A, Martins C, Rhoton AL Jr, de Oliveira E, Ribas GC (2008) Microsurgical anatomy and approaches to the cavernous sinus. Neurosurgery 62:1240–1263. https://doi.org/10.1227/01.neu.0000333790.90972.59
26. Marinkovic S, Gibo H, Vucevic R, Petrovic P (2001) Anatomy of the cavernous sinus region. J Clin Neurosci 8(Suppl 1):78–81. https://doi.org/10.1054/jocn.2001.0883
27. Dolenc VV (1989) Anatomy of the cavernous sinus. In: Dolenc VV (ed) Anatomy and Surgery of the Cavernous Sinus. Springer Vienna, Vienna, pp 3–137. https://doi.org/10.1007/978-3-7091-6942-1_2
28. Dolenc VV (1997) Transcranial epidural approach to pituitary tumors extending beyond the sella. Neurosurgery 41:542–550. https://doi.org/10.1097/00006123-199709000-00007 discussion 551–542
29. Bakhtiar Y, Hanaya R, Tokimura H, Hirano H, Oyoshi T, Fujio S, Bohara M, Arita K (2014) Geometric survey on magnetic resonance imaging of growth hormone producing pituitary adenoma. Pituitary 17:142–149. https://doi.org/10.1007/s11102-013-0479-z
30. Micko AS, Wöhrer A, Wolfsberger S, Knosp E (2015) Invasion of the cavernous sinus space in pituitary adenomas: endoscopic verification and its correlation with an MRI-based classification. J Neurosurg 122:803–811. https://doi.org/10.3171/2014.12.Jns141083
31. Zada G, Lin N, Laws ER Jr (2010) Patterns of extrasellar extension in growth hormone-secreting and nonfunctional pituitary macroadenomas. Neurosurg Focus 29:E4. https://doi.org/10.3171/2010.7.Focus10155
32. Dickerman RD, Oldfield EH (2002) Basis of persistent and recurrent Cushing disease: an analysis of findings at repeated pituitary surgery. J Neurosurg 97:1343–1349. https://doi.org/10.3171/jns.2002.97.6.1343
33. Knosp E, Steiner E, Kitz K, Matula C (1993) Pituitary adenomas with invasion of the cavernous sinus space: a magnetic resonance imaging classification compared with surgical findings. Neurosurgery 33:610–617. https://doi.org/10.1227/00006123-199310000-00008 discussion 617–618
34. Griessenauer CJ, Yalcin B, Matusz P, Loukas M, Kulwin CG, Tubbs RS, Gadol AA (2015) Analysis of the tortuosity of the internal carotid artery in the cavernous sinus. Child's Nerv Syst 31:941–944. https://doi.org/10.1007/s00381-015-2674-x
35. Inoue T, Rhoton AL Jr, Theele D, Barry ME (1990) Surgical approaches to the cavernous sinus: a microsurgical study. Neurosurgery 26:903–932
36. Ceylan S, Anik I, Cabuk B, Caklili M, Anik Y (2019) Extension pathways of pituitary adenomas with cavernous sinus involvement and its surgical approaches. World Neurosurg 127:e986–e995. https://doi.org/10.1016/j.wneu.2019.04.013
37. Lang J (1994) Hypophyseal ligaments. Acta Neurochir 130:144–146. https://doi.org/10.1007/bf01405514